Acta Cryst. (1998). D**54**, 501–509

Structure of d(CACGCG)·d(CGCGTG) in Crystals Grown in the Presence of Ruthenium^{III} Hexammine Chloride

P. Karthe and N. Gautham*

Department of Crystallography and Biophysics, University of Madras, Guindy Campus, Chennai 600 025, India. E-mail: crystal@giasmd01.vsnl.net.in

(*Received 26 May 1997; accepted 17 October 1997*)

Abstract

Hexammine ions are strong inducers of the transition from the B-form to the left-handed Z-form in DNA. Here the structure of d(CACGCG)·d(CGCGTG) obtained from crystals grown from a drop containing $[Ru(NH_3)_6]Cl_3$ is reported. The structure is clearly characterized as Z-DNA. When compared with the structure of d(CACGCG)·d(CGCGTG)/$MgCl_2$ and that of $d(CGCGCG)_2$, subtle differences are seen, most noticeably in the water structure. Since stable well diffracting crystals grow easily in the presence of $[Ru(NH_3)_6]Cl_3$ and since this ion is not visible in the electron density it is concluded that the ion plays a non-specific role in stabilizing Z-DNA.

1. Introduction

It is well known that cobalt^{III} hexammine, $[Co(NH_3)_6]^{3+}$, induces a transition of the DNA conformation from the B-form to the Z-form (Winkle & Sheardy, 1990; Winkle *et al.*, 1991; Lu *et al.*, 1992) even at low concentrations (Behe & Felsenfeld, 1981). A crystal structure study of the complex of $d(CGCGCG)_2$ with $[Co(NH_3)_6]^{3+}$ showed that the hydrated ion bound to guanine and phosphate acceptor sites on the surface of the DNA helix (Gessner *et al.*, 1985). Since the Z-DNA helix has a flat surface instead of the major groove, it was concluded that a probable reason for the cobalt hexammine ion being a strong inducer of Z-DNA could be that the surface of Z-DNA permits the formation of several more hydrogen bonds to the ion than does B-DNA. The structure of $d(CGCGCG)_3$ complexed with $[Ru(NH_3)_6]^{3+}$ (Ho *et al.*, 1987) showed that though $[Ru(NH_3)_6]^{2+}$ is a weaker inducer of the B to Z transition as compared with $[Co(NH_3)_6]^{3+}$, the former was found bound to the helix more strongly than the latter.

In order to study the effect of ruthenium and cobalt hexammine ions on the stability of Z-DNA in the presence of A·T base pairs, crystals of d(CGCACG)·d(CGTGCG) and d(CACGCG)·d(CGCGTG) were grown in the presence of these and other ions. The structures of d(CGCACG)·d(CGTGCG) complexed with Ba^{2+} and d(CACGCG)·d(CGCGTG) with Mg^{2+} have been reported earlier (Sadasivan & Gautham, 1995). In this paper the structure of d(CACGCG)·d(CGCGTG) determined from crystals grown in the presence of $[Ru(NH_3)_6]Cl_3$ is reported.

Table 1. *Crystal data, data-collection and refinement parameters for HA2RU*

Crystal data	
Chemical formula	$C_{115}H_{135}O_{68}N_{47}P_{10}$
Molecular weight	3561
Crystal size (mm)	0.5 × 0.2 × 0.2
Crystal system, space group	Orthorhombic, $P2_12_12_1$
a (Å)	17.88 (1)
b (Å)	30.87 (1)
c (Å)	44.83 (1)
V (Å^3)	24606
Z	4
Data-collection parameters	
Radiation type, wavelength (Å)	Cu $K\alpha$, 1.5418
Temperature (K)	296
No. of reflections for cell parameters	25
θ range for cell parameters (°)	8–15
No. of independent reflections	3314
No. of observed reflections	2014
Observation criterion	$\geq 2\sigma(F_o)$
θ maximum (°)	28
Completeness of the data ($\geq 2\sigma$)	
Resolution range ($\sin\theta/\lambda$)	Completeness (%)
0.1000–0.1672	93.1
0.1672–0.2033	83.0
0.2033–0.2294	73.1
0.2294–0.2513	65.2
0.2513–0.2688	53.7
0.2688–0.2853	49.6
0.2853–0.3049	30.0
Refinement parameters	
Refinement on	F
Final R factor	0.193
Resolution range (Å)	5–1.64
No. of reflections used in refinement	2014
No. of parameters refined	1108
Minimum isotropic temperature factor (Å^2)	2.0
Refinement method	Restrained least-squares (Hendrickson & Konnert, 1981)
Source of atomic scattering factors	*International Tables for X-ray Crystallography* (1974) Vol IV

Although the structure was refined to 19.3% at a resolution of 1.64 Å, the metal ion could not be located in the Fourier maps. This may indicate a non-specific charge neutralization role for $[Ru(NH_3)_6]Cl_3$ in stabilizing Z-DNA.

2. Experimental

2.1. *Crystallization and data collection*

Crystals were grown by vapour diffusion using the hanging-drop method. A drop containing 1 m*M* of the hexamer duplex, 50 m*M* sodium cacodylate buffer at pH 6.9, 1 m*M* spermine and 1 m*M* $[Ru(NH_3)_6]Cl_3$ was equilibrated at room temperature (296 K) against 50% 2-methyl-2,4-pentanediol in the reservoir. Hexagonal crystals of length greater than 0.3 mm were obtained after eight weeks.

A crystal of length 0.5 mm and diameter 0.2 mm was used for X-ray data collection. The intensity data were collected at 296 K on an Enraf–Nonius CAD-4 diffractometer with graphite-monochromated Cu $K\alpha$ radiation (λ = 1.5418 Å), at 40 kV, 32 mA setting. The lattice parameters were obtained from a least-squares fit of 25 reflections in the range $8 \leq \theta \leq 15^\circ$. The crystal belongs to the orthorhombic system, with cell parameters a = 17.88 (1), b = 30.87 (1) and c = 44.83 (1) Å; space group $P2_12_12_1$. The crystal diffracted to a resolution of 1.64 Å ($2\theta = 56^\circ$). The data were collected over an octant of the reflection sphere with $0 \leq h \leq 11$, $0 \leq k \leq 19$, $0 \leq l \leq 27$. A total of 3314 unique reflections were recorded. Three standard reflections were monitored every hour for crystal decay, and showed no significant change in intensity over the period of data collection. In order to check for absorption effects and to apply an absorption correction if necessary, the reflections (1 3 0), (1 6 0) and (2 7 0) with $\chi \simeq 90^\circ$ were measured at different values of ψ as suggested by North *et al.* (1968). The ratio of minimum to maximum intensity was 0.55; therefore, an empirical absorption correction (North *et al.*, 1968) was applied in addition to Lorentz and polarization corrections.

2.2. *Structure solution and refinement*

The structure was solved by the molecular replacement method. The coordinates of the d(CACGCG)·d(CGCGTG) duplex from the magnesium structure were used as the starting model. The program *ULTIMA* (Rabinovich & Shakked, 1984) was used for rotation–translation search. The molecular replacement solution was refined initially as a rigid body with the program *CORELS* (Sussman *et al.*, 1977) using 10–4 Å resolution data. After eight cycles of refinement the R factor was 0.297. Further restrained least-squares refinement of individual atomic positions was carried out using *NUCLSQ* (Westhof *et al.*, 1985) and the R factor dropped to 0.18. The refinement proceeded by adding higher angle data step-by-step to the maximum resolution of 1.64 Å. At this point electron-density maps with coefficients $(2F_o - F_c)$ and $(F_o - F_c)$ were calculated with the phases derived from the refined coordinates and displayed using *FRODO* (Jones, 1978). The model fitted well with the electron density and only small changes were found necessary. Based on a 1.64 Å map, initially five water molecules were added. Small and well defined spheres of electron density at the 2.5σ level in $(F_o - F_c)$ maps and 1σ level in $(2F_o - F_c)$ maps were considered as water molecules, provided they could not be explained by the atoms of the DNA

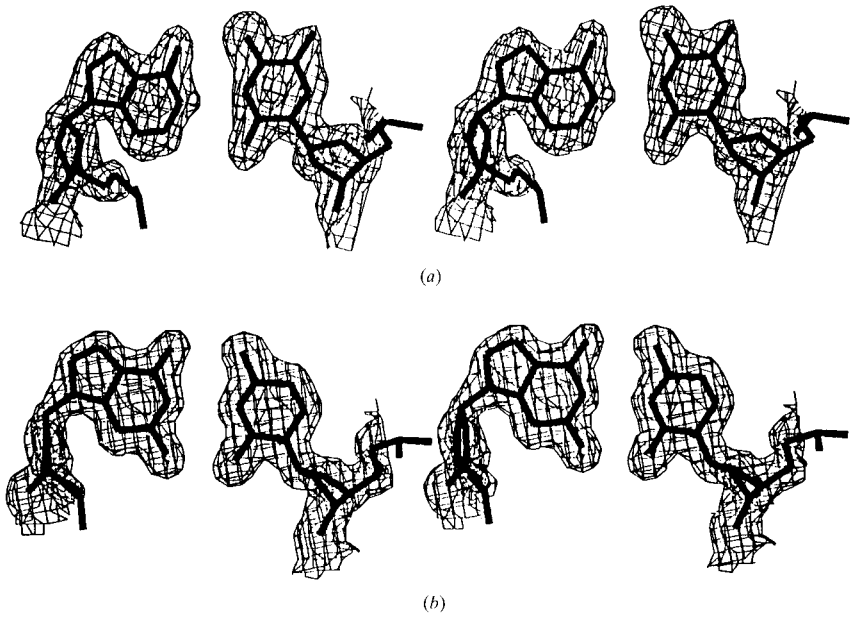

Fig. 1. (*a*) The $2F_o - F_c$ electron-density map around A2·T11 base pair. The electron density is contoured at 1.0σ level. The bases are indicated by thick lines. (*b*) The C3·G10 base pair superimposed on a section of a $2F_o - F_c$ electron-density map contoured at 1.0σ level. All other C·G base pairs in the molecule show closely similar electron density.

Table 2. *Statistics from the final cycle of NUCLSQ refinement for HA2RU*

Restraint groups and parameters	Standard deviation	R.m.s. deviation	Weight applied to restraints
Distance restraints (Å)			
Sugar/base bond distances	0.02	0.02	300
Sugar/base bond angles	0.04	0.05	150
Phosphate bond distances	0.04	0.106	150
Phosphate bond angles	0.04	0.06	150
Plane restraints (Å)	0.02	0.019	250
Chiral volume restraints (Å)	0.03	0.084	83.33
Non-bonded contact restraints (Å)			
Single torsions	0.06	0.135	16.0
Multiple torsions	0.06	0.277	16.0
Restraints on the isotropic thermal parameters (Å^2) of a pair of atoms related by			
Sugar/base bond distances	4	11	0.100
Sugar/base bond angles	6	12	0.100
Phosphate bond distances	8	13	0.100
Phosphate bond angles	10	14	0.100
Weighting scheme applied to the structure factors			
Weight = [AFSIG + BFSIG × (STHOL-0.1666667)]^2 where AFSIG = 1.000, BFSIG = 0.5000, STHOL = $\sin\theta/\lambda$			

Table 3. *Twist, rise, tilt, roll and slide in HA2RU, HA2MG and d(CG)$_3$*

Notable differences are shown in bold. All the helical parameters were calculated using *NEWHEL*91 (R. E. Dickerson, personal communication).

Sequence	Dinucleotide step	Twist (°)	Rise (Å)	Tilt (°)	Roll (°)	Slide (Å)
HA2RU	C1-A2·T11-G12	**−9.4**	3.80	−1.4	−4.8	−5.13
HA2MG	C1-A2·T11-G12	**−8.1**	3.84	−1.6	−2.4	−5.15
d(CG)$_3$	C1-G2·C11-G12	**−7.5**	3.95	−1.6	−4.1	−5.28
HA2RU	A2-C3·G10-T11	−48.2	3.62	−0.8	0.8	0.93
HA2MG	A2-C3·G10-T11	−49.4	3.75	0.6	1.5	0.64
d(CG)$_3$	G2-C3·G10-C11	−49.8	3.90	−2.8	−0.1	0.75
HA2RU	C3-G3·G9-G10	−11.0	3.78	0.0	−3.1	−5.22
HA2MG	C3-G3·C9-G10	−10.3	3.65	−1.0	−3.7	−5.35
d(CG)$_3$	C3-G4·C9-G10	−8.0	3.57	0.2	−4.4	−5.38
HA2RU	G4-C5·G8-C9	−47.6	3.71	1.7	**1.1**	0.63
HA2MG	G4-C5·G8-C9	−48.1	3.69	1.4	**3.5**	0.75
d(CG)$_3$	G4-C5·G8-C9	−52.0	3.65	0.2	1.7	0.59
HA2RU	C5-G6·C7-G8	−14.0	3.74	−0.9	**−0.8**	−5.09
HA2MG	C5-G6·C7-G8	−13.6	3.75	−0.2	**−2.7**	−5.50
d(CG)$_3$	C5-G6·C7-G8	−9.6	4.06	2.3	0.7	−5.07

molecules, and it was possible to form hydrogen bonds with the polar atoms of the helix or with other water molecules. The temperature factors of the water molecules were monitored to ensure that they stayed within acceptable limits (less than 50 Å^2). In each cycle two or three water molecules were added and a total of 37 were identified. Great care was exercised in the interpretation of the solvent electron density and the maps were constantly searched for possible metal ion sites. Until the end, however, it was not possible to see any density corresponding to $[Ru(NH_3)_6]Cl_3$. The final R factor is 0.193 for 2014 reflections with $F_o \geq 2\sigma(F_o)$ in the 5–1.64 Å resolution shell with a correlation coefficient of 0.97. The final difference Fourier map was free of gross unexplained features. The electron density around the base pair A2·T11 is shown in Fig. 1(*a*) and that around the G4·C9 base pair is shown in Fig. 1(*b*). Crystal data, data-collection parameters and refinement parameters are given in Table 1. Weights and other statistical parameters from the final cycle of *NUCLSQ* refinement are given in Table 2. The average B value for the bases (15.7 Å^2) is nearly same as that of the sugars (15.5 Å^2) and lower than that of the phosphates (27.9 Å^2). In general, the present structure exhibits slightly higher temperature factors than the magnesium structure even though in both cases the data were collected at approximately the same temperature (Sadasivan & Gautham, 1995). The B factors for the solvent molecules vary from 18.3 to 43.1 Å^2 with an average of 32.2 Å^2. The coordinates and the structure factors have been deposited in the Nucleic Acid Database.†

† Atomic coordinates and structure factors have been deposited with the Nucleic Acid Database (Reference: ZDF059). Free copies may be obtained through The Managing Editor, International Union of Crystallography, 5 Abbey Square, Chester CH1 2HU, England (Reference: VJ0009).

Table 4. *Propeller twist, buckle, inclination, tip, x-displacement (x-dis) and y-displacement (y-dis) in HA2RU, HA2MG and d(CG)$_3$*

Notable differences are shown in bold.

Sequence	Base pair	Propeller twist (°)	Buckle (°)	Inclination (°)	Tip (°)	*x*-dis (Å)	*y*-dis (Å)
HA2RU	C1·G12	−0.6	−3.9	−6.0	**5.3**	3.20	3.66
HA2MG	C1·G12	−0.1	−3.2	−6.0	**2.1**	2.86	3.50
d(CG)$_3$	C1·G12	−0.5	−0.5	−8.2	**7.2**	2.83	3.92
HA2RU	A2·T11	**0.0**	4.5	−4.6	0.6	2.67	−1.13
HA2MG	A2·T11	**−1.8**	5.6	−4.5	−0.2	2.49	−0.92
d(CG)$_3$	G2·C11	**−3.4**	6.2	−6.7	3.2	2.26	−0.54
HA2RU	C3·G10	0.5	**0.2**	3.9	1.3	2.10	2.53
HA2MG	C3·G10	−0.5	**−7.4**	−5.1	1.2	1.85	2.13
d(CG)$_3$	C3·G10	−6.0	**−4.3**	−3.9	3.1	1.36	2.33
HA2RU	G4·C9	**−4.5**	7.7	−3.9	−1.8	2.00	−2.64
HA2MG	G4·C9	**−2.1**	8.2	−4.1	−2.4	1.85	−2.64
d(CG)$_3$	G4·C9	**−0.1**	8.2	−4.1	−1.2	1.32	−2.64
HA2RU	C5·G8	−1.8	**−7.9**	−5.6	−0.6	3.15	**0.80**
HA2MG	C5·G8	−2.0	**−8.5**	−5.6	1.0	3.02	**0.74**
d(CG)$_3$	C5·G8	0.0	**0.2**	−4.3	0.4	2.65	**0.22**
HA2RU	G6·C7	−2.5	**2.6**	−4.7	−1.4	3.23	−3.85
HA2MG	G6·C7	−3.1	**3.2**	−5.4	−1.6	3.14	−3.74
d(CG)$_3$	G6·C7	4.8	**−5.4**	−6.6	1.1	2.94	−3.99
Mean		−1.6	0.5	−4.8	0.6	2.72	−0.10
Mean		−1.6	−0.4	−5.1	0.0	2.53	−0.16
Mean		−0.9	0.7	−5.6	2.3	2.23	−0.12

3. Results

In the present structure the nucleotides are labelled C1–G6 on the strand 1 and C7–G12 on the strand 2, both in the 5′ to 3′ direction. Henceforth, the present structure is referred to as HA2RU, and the structure of d(CACGCG)·d(CGCGTG)/$MgCl_2$ as HA2MG. Structural comparison is also made with d(CGCGCG)$_2$/$MgCl_2$ (Wang *et al.*, 1979) which has been taken to represent 'standard' Z-DNA and is henceforth called d(CG)$_3$. Fig. 2 is a superposition of HA2RU on HA2MG. The overall structure of HA2RU is very similar to the other Z-DNA hexanucleotides. However, a detailed comparison of HA2RU and HA2MG reveals differences between the two structures which might have resulted from the different metal ions used for crystallization.

Table 3 gives the values of the base-step parameters such as twist, rise, tilt, roll and slide. The dinucleotide repeat characteristic of Z-DNA is clearly visible. The average dinucleotide twist is −59.2°, almost the same as −59.5° observed in HA2MG. The twists at different steps show that the pyrimidine–purine steps in HA2RU

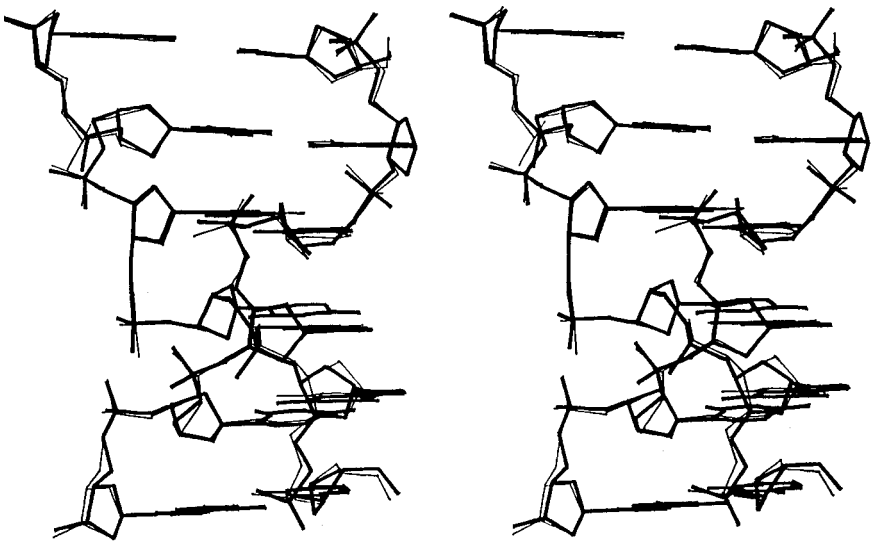

Fig. 2. Superposition of HA2RU (thick lines) on HA2MG (thin lines).

are slightly overwound as compared to HA2MG while the purine–pyrimidine steps are slightly underwound. They also indicate that HA2RU deviates more from the $d(CG)_3$ than HA2MG does. The average distance between the base pairs as measured along the helical axis (*i.e.* the rise, Table 3) is 3.73 Å, closely comparable with the value of 3.74 Å observed in HA2MG. Other parameters of the base steps such as tilt, roll and slide (Table 3) are also closely similar in the present structure and HA2MG. Like the base-step parameters, the base-pair parameters (Table 4) such as propeller twist, inclination, buckle *etc.*, show no remarkable differences. The values of x displacement are somewhat higher in HA2RU, indicating a shift of the base pairs away from the helix axis into the major groove. The extent of overlap between adjacent base pairs is slightly greater in HA2RU (Fig. 3).

The backbone torsion angles (Table 5) show that the major difference between HA2RU and HA2MG is at G4, where the differences in the angles α (O3′—P—O5′—C5′), γ (O5′—C5′—C4′—C3′) and δ (C5′—C4′—C3′—O3′) are almost 30°. The glycosidic torsion angles clearly follow the alternating *anti*, *syn* pattern for pyrimidines and purines, respectively, characteristic of Z-DNA. A noticeable conformational difference between the present structure and HA2MG and $d(CG)_3$ shows up in the sugar puckering (Table 5). In Z-DNA, the purines are associated with C3′-*endo* sugar puckers and the pyrimidines with C2′-*endo* sugars. Neither HA2RU nor HA2MG follows this pattern entirely. The sugar puckers of the C1, C7 and G8 residues in HA2RU are C2′-*endo*, C1′-*exo* and C1′-*exo*, respectively, in comparison with the C3′-*exo*, C2′-*endo* and C4′-*exo* puckers found in the analogous residues of the HA2MG.

The molecule has a deep minor groove and a flat major groove. Examination of the cross-strand (G6–G10 and G4–G12) phosphorous–phosphorous distances (diminished by 5.8 Å to account for the size of the phosphate group) in HA2RU suggests that width of the minor groove is slightly decreased when compared with

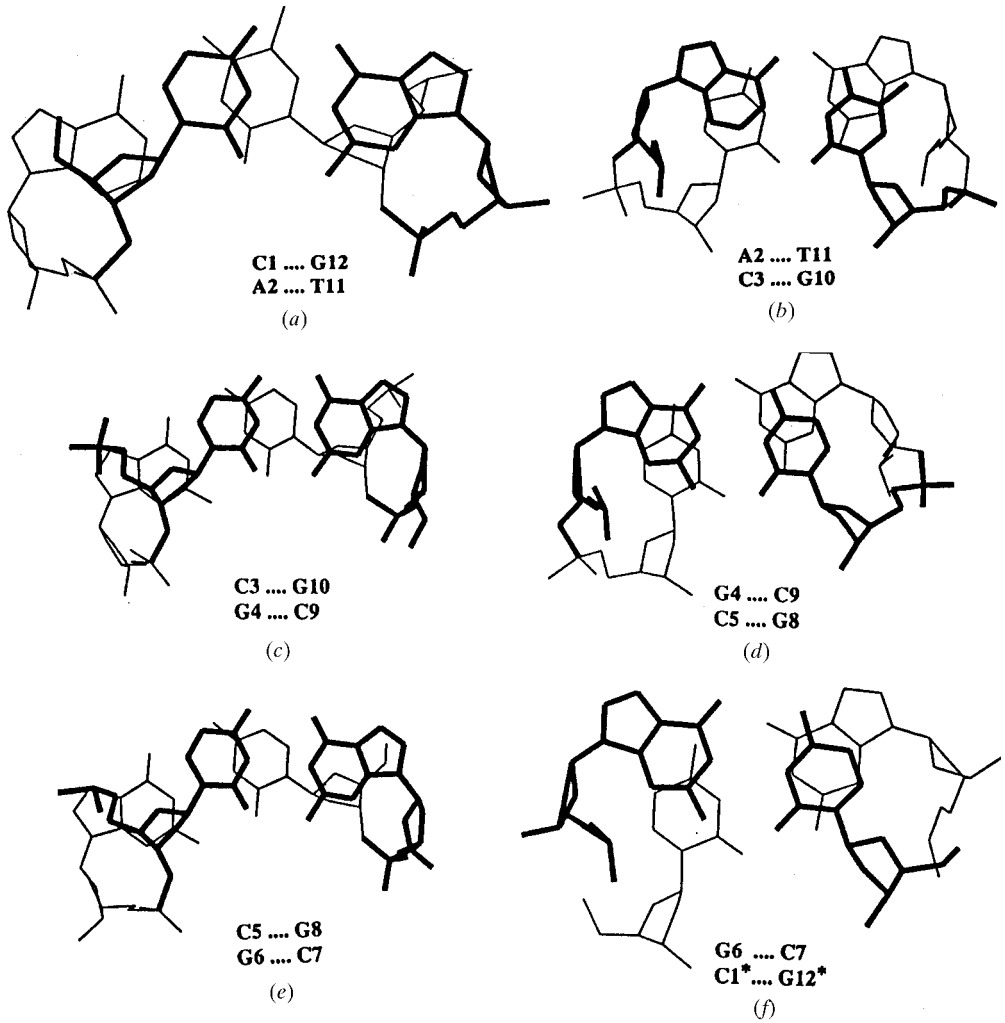

Fig. 3. The stacking of adjacent base pairs. View along the helix axis. * indicates bases belonging to the 2_1 screw symmetry-related molecules.

Table 5. *Backbone and glycosyl torsion angles and ribose pseudorotation parameters (°) in HA2RU, HA2MG and d(CG)$_3$*

Parameters for HA2RU, HA2MG and d(CG)$_3$ are shown on the first, second and third lines respectively. Notable differences are shown in bold.

Residue	α	β	γ	δ	ε	ζ	χ	P	τ_m	Puckering type
C1			**103**	**141**	278	49	**210**	**167**	37	**C2′-***endo*
C1			**22**	**156**	275	50	**223**	**190**	43	**C3′-***exo*
C1			**47**	144	267	81	**208**	**154**	35	C2′-*endo*
A2	97	**160**	164	93	232	**321**	60	47	29	**C4′-***exo*
A2	98	**181**	164	94	232	**306**	61	49	30	**C4′-***exo*
G2	63	186	174	94	240	294	57	30	38	**C3′-***endo*
C3	179	225	72	128	**256**	**87**	215	143	38	C2′-*endo*
C3	180	223	72	139	**271**	**67**	206	151	45	C2′-*endo*
C3	216	234	50	152	**258**	**76**	202	148	37	C2′-*endo*
G4	**69**	176	**177**	**104**	**243**	**301**	53	34	12	**C3′-***endo*
G4	**95**	184	**151**	**81**	**228**	**317**	62	41	37	**C4′-***exo*
G4	**70**	188	**177**	**95**	**181**	**65**	52	30	32	C3′-*endo*
C5	204	209	**73**	137	261	67	193	146	49	C2′-*endo*
C5	209	211	**52**	139	254	71	204	149	43	C2′-*endo*
C5	169	167	**43**	142	267	74	215	155	38	C2′-*endo*
G6	**63**	179	**203**	136			66	170	27	C2′-*endo*
G6	**88**	174	**179**	145			76	170	36	C2′-*endo*
G6	**74**	178	**180**	149			78	170	36	C2′-*endo*
C7			54	123	**253**	80	203	131	52	**C1′-***exo*
C7			57	134	**274**	69	208	145	42	**C2′-***endo*
C7			53	147	**270**	78	218	154	38	C2′-*endo*
G8	**58**	180	188	**125**	227	**308**	67	**122**	25	**C1′-***exo*
G8	**72**	193	175	**99**	239	**319**	66	**63**	20	**C4′-***exo*
G8	61	187	175	**95**	244	**286**	70	**29**	33	**C3′-***endo*
C9	213	210	49	150	264	67	217	177	50	C2′-*endo*
C9	212	206	43	146	267	73	214	168	43	C2′-*endo*
C9	220	225	55	149	262	80	200	154	39	C2′-*endo*
G10	67	188	177	91	242	291	62	33	31	C3′-*endo*
G10	70	190	170	87	244	291	65	37	31	C3′-*endo*
G10	64	179	179	103	248	290	65	18	26	C3′-*endo*
T11	**211**	**200**	61	137	250	68	210	163	48	C2′-*endo*
T11	**195**	**231**	62	128	257	81	208	151	38	C2′-*endo*
C11	212	**236**	50	143	262	72	204	147	42	C2′-*endo*
G12	**94**	175	173	146			73	166	47	C2′-*endo*
G12	**75**	172	185	151			73	172	39	C2′-*endo*
G12	**74**	184	186	149			79	167	45	C2′-*endo*

Table 6. *Water–base sugar contacts*

pyr = pyrimidine and pur = purine.

Atom type	Number of contacts HA2RU	HA2MG
O2 (pyr)	3	6
N4 (pyr)	1	2
O6 (pur)	1	3
N2 (pur)	2	7
N7 (pur)	2	5
P, O1P, O2P	19	16
O5′	2	5
O3′	3	4
O4′	1	1

HA2MG. In HA2RU the P—P distance between G6–G10 residues is 1.99 Å and between G4–G12 it is 2.72 Å. But in HA2MG the corresponding values are 2.49 and 2.86 Å, respectively.

The organization of water molecules in the present structure is different from that in HA2MG. Table 6 gives the number of water contacts (within 3.4 Å) made by base and sugar atoms of HA2RU. For comparison, such contacts in HA2MG are also given. Out of a total of 34 contacts in HA2RU, 15 are also found in HA2MG. The spine of hydration with water molecules bridging the cytosine O2 groups, which is typically found in alternating dC–dG structures (Wang *et al.*, 1979; Gessner *et al.*, 1985, 1989; Egli *et al.*, 1991), is not present in HA2RU, but is partially observed in HA2MG (C1 O2···3.44 Å···HOH6···3.59 Å···T11 O2···2.79 Å··· HOH 13···2.63 Å···C3 O2). There are six water–DNA contacts around the A·T base pair in both HA2RU and HA2MG. But the hydration pattern is different as can be seen from the Figs. 4(*a*) and 4(*b*). The A·T base pair is relatively sparsely hydrated as compared with the C·G base pairs. A similar situation has earlier been reported for d(CGCACG)·d(CGTGCG) (Sadasivan & Gautham, 1995) although not in HA2MG. The solvent structure around the C·G base pairs is also different in the two structures. For example the cross-strand water bridge involving the C3 O2 and the G10 N2 atoms (C3 O2···2.63 Å···HOH 13···3.35 Å···G10 N2) in

Table 7. *Hydration of phosphates in HA2RU and HA2MG*

Phosphate	HA2RU	Distances (Å)	HA2MG	Distance (Å)
2P	O2P···HOH 18	3.05		
	O2P···HOH 37	3.08		
3P	O1P···HOH 19	2.17	P···HOH 17	3.32
			O1P···HOH 9	3.17
			O1P···HOH 11	3.21
4P	O1P···HOH 36	3.20	O2P···HOH 15	2.83
	O2P···HOH 33	3.04		
5P	O1P···HOH 43	3.36	O1P···HOH 36	3.28
	O2P···HOH 43	3.31		
6P	O2P···HOH 48	2.87	O1P···HOH 26	3.01
8P	O2P···HOH 35	3.01	O1P···HOH 41	2.88
	O2P···HOH 38	2.88	O2P···HOH 20	3.40
9P			O2P···HOH 40	2.90
			O1P···HOH 30	2.60
10P	O2P···HOH 21	3.17	O2P···HOH 29	2.98
	O1P···HOH 37	2.80		
	O1P···HOH 14			
11P	O2P···HOH 15	3.12	P···HOH 10	3.22
	O1P···HOH 25	3.40	O2P···HOH 10	2.65
	O1P···HOH 40	3.39		
12P			O1P···HOH 7	3.34

HA2MG is not observed in HA2RU. Similarly an intraresidue water contact (C3 O3′···2.94 Å···HOH 15 ···3.48 Å···HOH 6···2.63 Å···C3 O2) involving the O3′ and the O2 atoms of C3 residue is present only in HA2MG. However, an intrabase water contact is observed in both HA2RU (G10 O6···HOH 26··· G10 N7) and HA2MG (G10 O6···HOH 14···G10 N7). Similar differences are seen around the other C·G base pairs. The water structure around the negatively charged phosphate groups (Table 7) is also different in the two structures. For example in HA2RU the phosphate group of the A2 residue makes two water contacts whereas in HA2MG it is not hydrated. Similarly the phosphate group of C9 residue is not hydrated in HA2RU, while in the analogous residue in HA2MG it has two water contacts. Most of the water molecules are involved in multiple contacts. A few base–base, phosphate–base and phosphate–phosphate intrahelical water bridges are present. In general, the water molecules make a more intricate network of contacts in HA2MG than in HA2RU.

4. Discussion

As expected, the present structure is closely similar to previously reported Z-DNA structures obtained from a variety of studies (Wang *et al.*, 1979; Arnott *et al.*, 1980; Gupta *et al.*, 1980; Mitra *et al.*, 1981; Rich *et al.*, 1984; Ho & Mooers, 1997). Unlike the case of A or B forms, Z-DNA has only a couple of examples of sequence-dependent microheterogenity (Coll *et al.*, 1988; Sadasivan & Gautham, 1995). Crystals of several different sequences grown in a variety of conditions assume almost identical left-handed double-helical structures (Ho & Mooers, 1997). It has been shown that even the

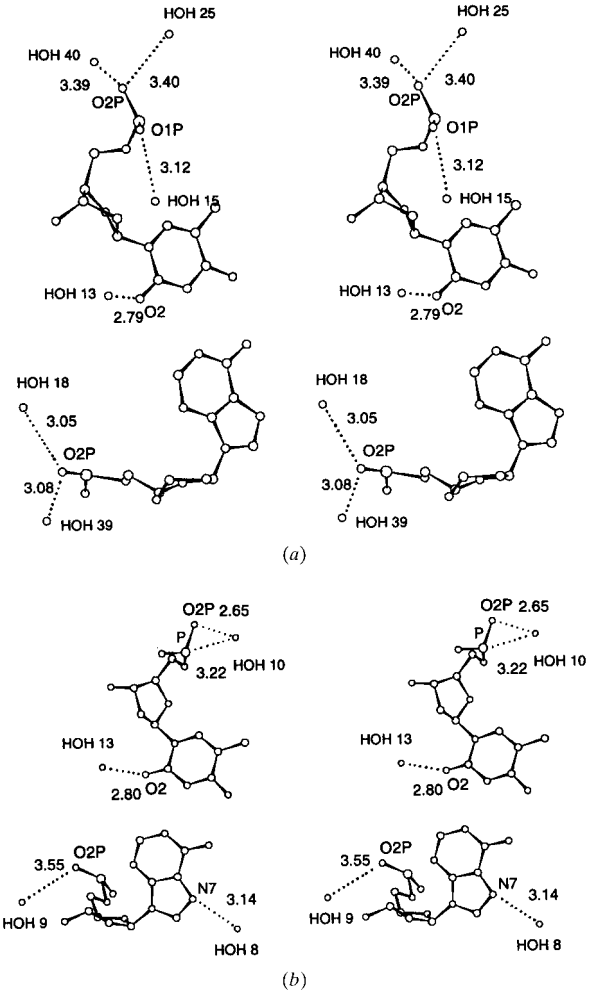

Fig. 4. Stereoview of water contacts around the A2·T11 base pair in (*a*) HA2RU and (*b*) HA2MG.

absence of high salt, earlier thought to be necessary (Pohl & Jovin, 1972; Thaman *et al.*, 1981; Thomas & Peticolas, 1984), could be compensated by other factors such as methylation of cytosine (Behe & Felsenfeld, 1981; Malfoy *et al.*, 1982; Jovin *et al.*, 1983; Wang *et al.*, 1985). Hexammine salts are helix-stabilizing agents (Ascoli *et al.*, 1973; Eichorn, 1982; Hingerty *et al.*, 1982). They are especially strong inducers of Z-DNA (Winkle & Sheardy, 1990; Winkle *et al.*, 1991; Lu *et al.*, 1992), even in sequences that are not entirely alternating CG (Brennan *et al.*, 1986). The absence of electron density for $[Ru(NH_3)_6]Cl_3$ in the present structure is an indication that the ion plays a non-specific role in stabilizing the structure. This result is different from that obtained for the d(CGCGCG)$_2$/ruthenium^{III} hexammine complex (Ho *et al.*, 1987) where the ion makes direct and water-mediated contacts with atoms of the base as well as of the sugar–phosphate backbone. It may be noted that the d(CGCGCG)$_2$/ruthenium^{III} hexammine complex was prepared by allowing the ions to soak into crystals which had previously been prepared from a solution containing magnesium chloride. In the case of HA2RU, however, crystals were grown from a solution which contained $[Ru(NH_3)_6]Cl_3$ and no other metal ion, except a relatively low concentration of Na^+ in the buffer. It is not clear if this is the reason for the differences observed in the two structures. In a recent review on Z-DNA crystallography, Ho & Mooers (1997) showed that a major component of Z-DNA stabilization is the base-stacking interaction in the CpG dinucleotide. This is supported by the strucure of d(CG) (Ramakrishnan & Viswamitra, 1988) which crystallizes as Z-DNA. Sadasivan & Gautham (1995) showed that a change in the position of A·T base pair disrupts the DNA conformation and that the greater stability of d(CACGCG)·d(CGCGTG) as compared with d(CGCACG)·d(CGTGCG) was probably because of the presence of a continuous stretch of four C·G base pairs in the former sequence. The variations from regularity in the twist angle in the latter sequence are reflected in the pattern of the stacking of adjacent base pairs. Thus, the stability or otherwise of the Z-DNA hexamer was more due to the sequence and the base-stacking property of adjacent base pairs than to the metal ion present. The present work appears to confirm this hypothesis. Ho & Mooers (1997) also showed that the strength of the solvent interactions as calculated from solvent free energies contributes to the greater Z-DNA stability of d(CG) over d(AT). The relatively sparse hydration of the A·T base pair in the present structure could be related to this effect.

PK thanks CSIR, India for the award of Senior Research Fellowship. We thank Dr S. Krishnaswamy, Bioinformatics Centre, Madurai Kamaraj University, for useful discussions. We acknowledge with gratitude the use of the National High-Resolution Graphics Facility, Bioinformatics Centre, Madurai Kamaraj University. We thank DBT, India, for the financial support.

References

Arnott, S., Chandrasekaran, R., Birdsall, D. L., Leslie, A. G. W. & Ratliff, R. L. (1980). *Nature (London)*, **283**, 743–745.

Ascoli, F., Branca, C., Mancini, C. & Bispisa, B. (1973). *Biopolymers*, **12**, 2431–2434.

Behe, M. & Felsenfeld, G. (1981). *Proc. Natl Acad. Sci. USA*, **78**, 1619–1623.

Brennan, R. G., Westhof, E. & Sundaralingam, M. (1986). *J. Biomol. Struct. Dynam.* **3**, 649–665.

Coll, M., Fita, I., Lloveras, J. Subirana, J. A., Bardella, F., Huynh-Dinh, T. & Igolen, J. (1988). *Nucleic Acids. Res.* **16**, 8695–8705.

Eichorn, G. L. (1982). *Inorganic Biochemistry*, Vol. 4, p. 16. London: Bartholomew Press.

Egli, M., Williams, L. D., Gao, Q. & Rich, A. (1991). *Biochemistry*, **30**, 11388–11402.

Gessner, R. V., Frederick, C. A., Quigley, G. J., Rich, A. & Wang, A. H.-J. (1989). *J. Biol. Chem.* **264**, 7921–7935.

Gessner, R. V., Quigley, G. J., Wang, A. H.-J., van der Marel, G., van Boom, J. H. & Rich, A. (1985). *Biochemistry*, **24**, 237–240.

Gupta, G., Bansal, M. & Sasisekharan, V. (1980). *Proc. Natl Acad Sci. USA*, **77**, 6486–6490.

Hendrickson, W. A. & Konnert, J. H. (1981). *Biomolecular Structure, Function, Conformation and Evolution*, Vol. 1, edited by R. Srinivasan, E. Subramanian & N. Yathindra. pp. 43–67. Oxford: Pergamon Press.

Hingerty, B. E., Brown, R. S. & Klug, A. (1982). *Biochim. Biophys. Acta*, **697**, 78–82.

Ho, P. S., Frederick, C. A., Saal, D., Wang, A. H.-J. & Rich, A. (1987). *J. Biomol. Struct. Dynam.* **4**, 521–534.

Ho, P. S. & Mooers, B. H. M. (1997). *Biopolymers*, **44**, 1, 65–90.

International Tables for X-ray Crystallography (1974). Vol. IV, Kynoch Press, Birmingham, England.

Jones, A. (1978). *J. Appl. Cryst.* **11**, 268–272.

Jovin, T. M., McIntosh, L. P., Arndt-John, D. J., Zarling, D. A., Robert-Nicoud, M., van de Sande, J. H., Jorgenson, K. F. & Eckstein, F. (1983). *J. Biomol. Struct. Dynam.* **1**, 21–57.

Lu, M., Kallenbach, N. R. & Sheardy, R. D. (1992). *Biochemistry*, **31**, 4712–4719.

Malfoy, B., Rousscau, M. & Leng, M. (1982). *Biochemistry*, **21**, 5463–5467.

Mitra, C. K., Sarma, M. H. & Sarma, R. H. (1981). *Biochemistry*, **20**, 2036–2041.

North, A. C. T., Phillips, D. C. & Mathews, F. S. (1968). *Acta Cryst.* A**24**, 351–359.

Pohl, F. M. & Jovin, T. M. (1972). *J. Mol. Biol.* **67**, 375–396.

Rabinovich, D. & Shakked, Z. (1984). *Acta Cryst.* A**40**, 195–200.

Ramakrishnan, B. & Viswamitra, M. A. (1988). *J. Biomol. Struct. Dynam.* **6**, 511–523.

Rich, A., Nordheim, A. & Wang, A. H.-J. (1984). *Ann. Rev. Biochem.* **53**, 791–846.

Sadasivan, C. & Gautham, N. (1995). *J. Mol. Biol.* **248**, 918–930.

Sussman, J. L., Holbrook, S. R., Church, G. M. & Kim, S.-H. (1977). *Acta Cryst.* A**33**, 800–804.
Thaman, T. J., Lord, R. C., Wang, A. H.-J. & Rich, A. (1981). *Nucleic Acids Res.* **9**, 5443–5457.
Thomas, G. A. & Peticolas, W. L. (1984). *Biochemistry*, **23**, 3202–3207.
Wang, A. H.-J., Gessner, R. V., van der Marel, G., van Boom, J. H. & Rich, A. (1985). *Proc. Natl Acad. Sci. USA*, **82**, 3611–3615.
Wang, A. H.-J., Quigley, G. J., Kolpak, F. J., Crawford, J. L., van Boom, J. H, van der Marel, G. & Rich, A. (1979). *Nature (London)*, **282**, 680–686.
Westhof, E., Dumas, P. & Moras, D. (1985). *J. Mol. Biol.* **184**, 119–145.
Winkle, S. A., Aloyo, M. C., Morales, N., Zambrano, T. Y. & Sheardy, R. D. (1991). *Biochemistry*, **30**, 10601–10606.
Winkle, S. A. & Sheardy, R. D. (1990). *Biochemistry*, **29**, 6514.